

Influence of sintering temperature on microstructure and mixed electronic–ionic conduction properties of perovskite-type $\text{La}_{0.6}\text{Sr}_{0.4}\text{Co}_{0.8}\text{Fe}_{0.2}\text{O}_3$ ceramics

Qing Xu^{a,b,*}, Duan-ping Huang^a, Wen Chen^a, Joong-hee Lee^b, Bok-hee Kim^b,
Hao Wang^a, Run-zhang Yuan^a

^aState Key Laboratory of Advanced Technology for Materials Synthesis and Processing, Wuhan University of Technology,
Wuhan 430070, People's Republic of China

^bEngineering Research Institute, Chonbuk National University, Chonju 561756, South Korea

Received 3 February 2003; received in revised form 25 March 2003; accepted 28 May 2003

Abstract

Microstructural evolution and mixed electronic–ionic conduction properties of perovskite-type $\text{La}_{0.6}\text{Sr}_{0.4}\text{Co}_{0.8}\text{Fe}_{0.2}\text{O}_3$ ceramics were investigated in the sintering temperature range 1100–1250 °C. The results confirm the crucial role of sintering temperature on microstructure and mixed conduction properties. The improvement of the mixed conduction properties with the increased sintering temperature from 1100 to 1200 °C is ascribed to the development of densification. Further increase of the sintering temperature above 1200 °C declined the mixed conduction properties due to the generation of excessive liquid. With respect to the mixed conduction properties, the preferred sintering temperature was ascertained to be 1200 °C for $\text{La}_{0.6}\text{Sr}_{0.4}\text{Co}_{0.8}\text{Fe}_{0.2}\text{O}_3$ ceramics. The $\text{La}_{0.6}\text{Sr}_{0.4}\text{Co}_{0.8}\text{Fe}_{0.2}\text{O}_3$ ceramic sintered at 1200 °C exhibited an electrical conductivity of $1.26 \times 10^3 \Omega^{-1} \text{cm}^{-1}$ and an oxygen ionic conductivity of $3.73 \times 10^{-2} \Omega^{-1} \text{cm}^{-1}$ at 800 °C.

© 2003 Elsevier Ltd and Techna S.r.l. All rights reserved.

Keywords: A. Sintering; B. Microstructure; C. Electrical properties; D. Perovskites

1. Introduction

Perovskite-type complex oxides of $\text{La}_{1-x}\text{Sr}_x\text{Co}_{1-y}\text{Fe}_y\text{O}_3$ compositions are attracting growing attention because of their superior mixed electronic–ionic conduction properties. At elevated temperatures (about 800 °C), $\text{La}_{1-x}\text{Sr}_x\text{Co}_{1-y}\text{Fe}_y\text{O}_3$ compositions exhibit electronic conductivities exceeding $10^2 \Omega^{-1} \text{cm}^{-1}$ and ionic conductivities on the order of 10^{-2} – $1.0 \Omega^{-1} \text{cm}^{-1}$, making them promising candidate materials for many important applications, including cathodes for intermediate temperature solid oxide fuel cells, oxygen separation membranes, membrane reactors for syngas production and catalysts for oxidation of hydrocarbons [1–3]. The structure and electrical properties of the $\text{La}_{1-x}\text{Sr}_x\text{Co}_{1-y}\text{Fe}_y\text{O}_3$ oxides depend greatly on their composi-

tions. It was ascertained by Tai et al. that the solubility of Sr in the perovskite structure was limited to $x \leq 0.4$ and the variation of Co/Fe ratio also generated a significant influence on structure and electrical properties [4,5]. The $\text{La}_{1-x}\text{Sr}_x\text{Co}_{1-y}\text{Fe}_y\text{O}_3$ compositions have been extensively investigated, involving the electronic and ionic conduction characteristics [6,7], oxygen permeability [8], oxidation catalytic activity [9], etc. Considering the long-term stability of structure and properties during practical applications at elevated temperatures, most of these researches focused on the $\text{La}_{1-x}\text{Sr}_x\text{Co}_{1-y}\text{Fe}_y\text{O}_3$ compositions with a relatively low Co content such as $\text{La}_{0.6}\text{Sr}_{0.4}\text{Co}_{0.2}\text{Fe}_{0.8}\text{O}_3$. However, it has been confirmed that the $\text{La}_{1-x}\text{Sr}_x\text{Co}_{1-y}\text{Fe}_y\text{O}_3$ compositions with a relatively high Co content such as $\text{La}_{1-x}\text{Sr}_x\text{Co}_{0.8}\text{Fe}_{0.2}\text{O}_3$ were also viable candidate materials for applications at intermediate temperatures [6, 10].

The mixed electronic–ionic conduction properties of the $\text{La}_{1-x}\text{Sr}_x\text{Co}_{1-y}\text{Fe}_y\text{O}_3$ oxides were usually obtained

* Corresponding author. Tel.: +86-27-8764033; fax: +86-27-876-642079.

E-mail address: xuqing@mail.whut.edu.cn (Q. Xu).

from ceramic materials [6,7]. The effect of sintering temperature on the microstructure and mixed conduction properties of $\text{La}_{1-x}\text{Sr}_x\text{Co}_{1-y}\text{Fe}_y\text{O}_3$ ceramics is an intriguing subject of great importance, and was seldom reported. In this work, the microstructural evolution and mixed conduction properties of $\text{La}_{0.6}\text{Sr}_{0.4}\text{Co}_{0.8}\text{Fe}_{0.2}\text{O}_3$ ceramics were investigated in the sintering temperature interval 1100–1250 °C.

2. Experimental procedure

$\text{La}_{0.6}\text{Sr}_{0.4}\text{Co}_{0.8}\text{Fe}_{0.2}\text{O}_3$ powder was synthesized by a citrate method. Reagent grade $\text{La}(\text{NO}_3)_3 \cdot 6\text{H}_2\text{O}$, $\text{Sr}(\text{NO}_3)_2$, $\text{Fe}(\text{NO}_3)_3 \cdot 9\text{H}_2\text{O}$, $\text{Co}(\text{NO}_3)_2 \cdot 6\text{H}_2\text{O}$ and citric acid were used as starting materials. The nitrates were weighed according to the nominal composition of $\text{La}_{0.6}\text{Sr}_{0.4}\text{Co}_{0.8}\text{Fe}_{0.2}\text{O}_3$, and then dissolved into deionized water in a beaker. A designed amount of citric acid was added, and the mole ratio of citric acid to total metal cation content was 1.2. The pH of the yielded precursor solution was adjusted to 9–10 by NH_4OH solution to prevent precipitation. The solution was dehydrated using a vacuum oven to form sol and gel. The resulting gel was pulverized and calcined at 700 °C for 1 h. A single-phase perovskite structure with rhombohedral symmetry was identified for the calcined powder by X-ray diffraction (XRD). Scanning electron microscope (SEM) analysis shows that the powder consists of homogeneous particles with a main size distribution in 100–200 nm. The sub-micron powder was uniaxially pressed into rectangular bars ($30 \times 4 \times 4 \text{ mm}^3$) and disks (13 mm diameter and 2 mm thickness), respectively, followed by sintering at 1100–1250 °C for 4 h in air.

After etching in diluted hybrid acids, fractured cross sections of sintered specimens were investigated by SEM (Jeol JMS-5610LV). The ceramic specimens were polished to ensure surface flatness. The rectangular specimens were painted with platinum paste for measuring electrical conductivity. The electrical conductivity was then measured at 20–900 °C by a dc four-terminal method in air. Adopting the two-terminal blocking electrode method described by Chen et al. [7], the oxygen ionic conductivity was measured using disk specimens by a TH2816 high frequency precision LCR digital bridge (Chongzhou Tonghui Electronic Co. Ltd., China) at 400–800 °C in air.

3. Results and discussion

Fig. 1 shows the linear shrinkage and average grain size of $\text{La}_{0.6}\text{Sr}_{0.4}\text{Co}_{0.8}\text{Fe}_{0.2}\text{O}_3$ ceramics as a function of sintering temperature, indicating a slight increase of linear shrinkage from 21.6 to 22.8% and a considerable

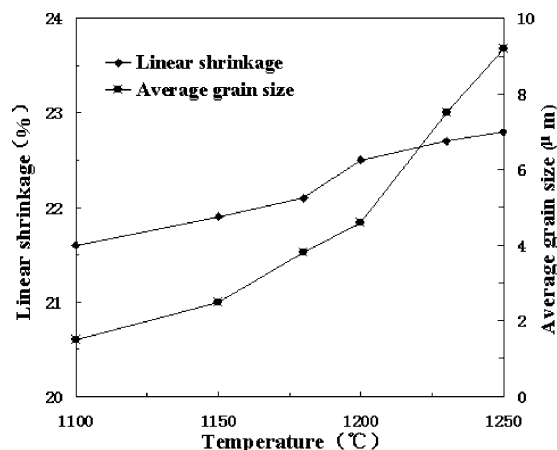


Fig. 1. Linear shrinkage and average grain size of $\text{La}_{0.6}\text{Sr}_{0.4}\text{Co}_{0.8}\text{Fe}_{0.2}\text{O}_3$ ceramics as a function of sintering temperatures.

increase of average grain size from 1.5 to 9.2 μm with the elevation of sintering temperature. Fig. 2 shows the SEM micrographs of $\text{La}_{0.6}\text{Sr}_{0.4}\text{Co}_{0.8}\text{Fe}_{0.2}\text{O}_3$ ceramics sintered at different temperatures. A porous microstructure with small grain size was observed in the specimen sintered at 1100 °C. The increase of sintering temperature significantly promoted the grain growth and microstructural densification. Compared with the gradual increase of grain size with sintering temperature in the range of 1100–1200 °C, there is a facilitated grain growth in the specimens sintered at 1230 and 1250 °C, respectively, implying a considerable increase in the amount of liquid after 1200 °C.

Fig. 3 shows the electrical conductivity (denoted as σ_e) of $\text{La}_{0.6}\text{Sr}_{0.4}\text{Co}_{0.8}\text{Fe}_{0.2}\text{O}_3$ ceramics as a function of measuring temperature. Due to the low oxygen ionic transport number in the $\text{La}_{1-x}\text{Sr}_x\text{Co}_{1-y}\text{Fe}_y\text{O}_3$ oxides (generally less than 1%), the electrical conductivity measured by the dc four-terminal method can be regarded as the representative of electronic conductivity [6]. The electrical conductivities of the specimens sintered at different temperatures display an identical variation with measuring temperature, increasing with measuring temperature through a maximum value near 600 °C and then decreasing. In the case of a same measuring temperature, the electrical conductivity increases with the sintering temperature from 1100 to 1200 °C and attains the largest value at 1200 °C, followed by a decrease of electrical conductivity with further elevated sintering temperature. Fig. 4 shows the plots of $\ln \sigma_e T$ versus $1000/T$ for $\text{La}_{0.6}\text{Sr}_{0.4}\text{Co}_{0.8}\text{Fe}_{0.2}\text{O}_3$ ceramics sintered at different temperatures. The plots are nearly linear at low temperatures, suggesting that small polaron hopping is the predominant mechanism for electronic conduction, expressed as [6]:

$$\sigma_e = (C/T)\exp(-E_a/KT) \quad (1)$$

where C is a material constant containing the carrier concentration term, T is the absolute temperature, E_a is

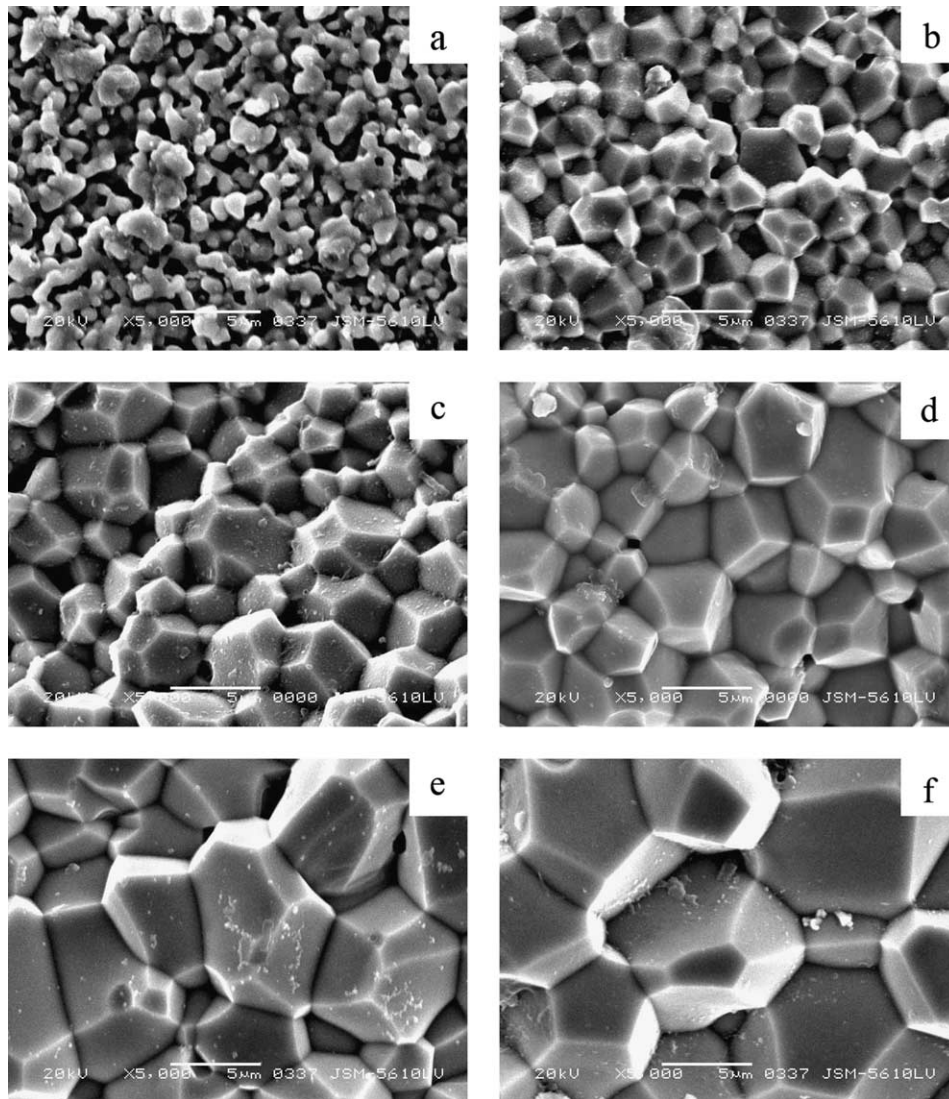


Fig. 2. SEM micrographs of $\text{La}_{0.6}\text{Sr}_{0.4}\text{Co}_{0.8}\text{Fe}_{0.2}\text{O}_3$ ceramics sintered at (a) 1100 °C, (b) 1150 °C, (c) 1180 °C, (d) 1200 °C, (e) 1230 °C, and (f) 1250 °C.

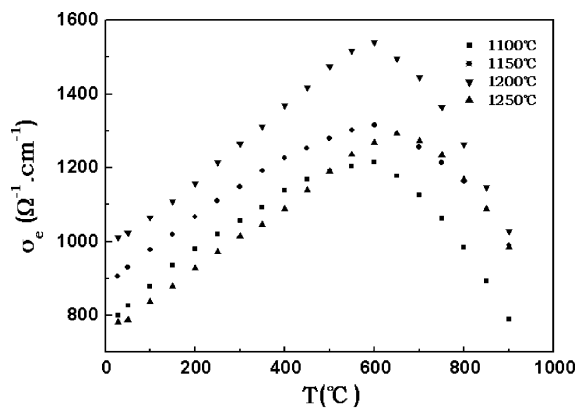


Fig. 3. Electrical conductivity (σ_e) of $\text{La}_{0.6}\text{Sr}_{0.4}\text{Co}_{0.8}\text{Fe}_{0.2}\text{O}_3$ ceramics as a function of measuring temperature.

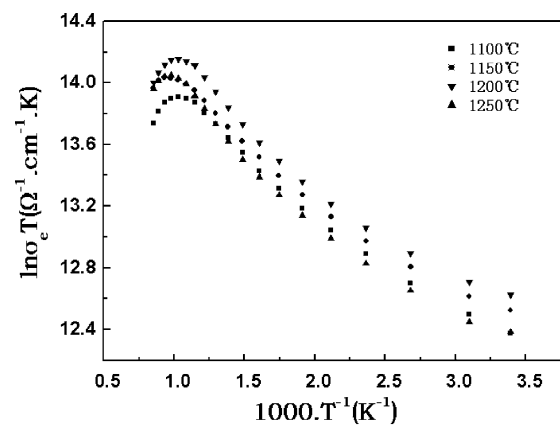


Fig. 4. Plots of $\ln \sigma_e T$ versus $1000/T$ for $\text{La}_{0.6}\text{Sr}_{0.4}\text{Co}_{0.8}\text{Fe}_{0.2}\text{O}_3$ ceramics sintered at different temperatures.

the activation energy for small polaron hopping, and K is the Boltzmann constant. At higher temperatures, the plots present a significant negative deviation from linearity. It is attributed to a substantial increase of thermally-induced oxygen loss, decreasing not only the concentration but also the mobility of electronic carrier [5].

Fig. 5 shows the temperature dependence of oxygen ionic conductivity (denoted as σ_{ion}) for $\text{La}_{0.6}\text{Sr}_{0.4}\text{Co}_{0.8}\text{Fe}_{0.2}\text{O}_3$ ceramics sintered at different temperatures. The Arrhenius plots over the whole measuring temperature range yielded straight lines. At an identical measuring temperature, the ionic conductivity shows a rather similar variation with sintering temperature to that of the electrical conductivity, with the specimen sintered at 1200 °C approaching the highest ionic conductivity as well.

The oxygen ionic transport numbers were calculated by dividing the oxygen ionic conductivity by the electrical conductivity. Fig. 6 shows the ionic transport numbers of $\text{La}_{0.6}\text{Sr}_{0.4}\text{Co}_{0.8}\text{Fe}_{0.2}\text{O}_3$ ceramics sintered at different temperatures. In the case of the ionic transport

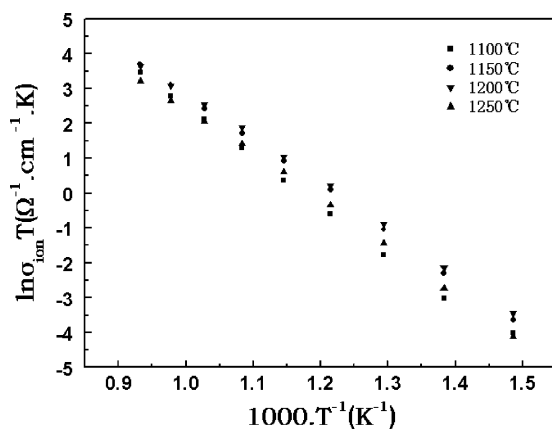


Fig. 5. Temperature dependence of oxygen ionic conductivity (σ_{ion}) for $\text{La}_{0.6}\text{Sr}_{0.4}\text{Co}_{0.8}\text{Fe}_{0.2}\text{O}_3$ ceramics sintered at different temperatures.

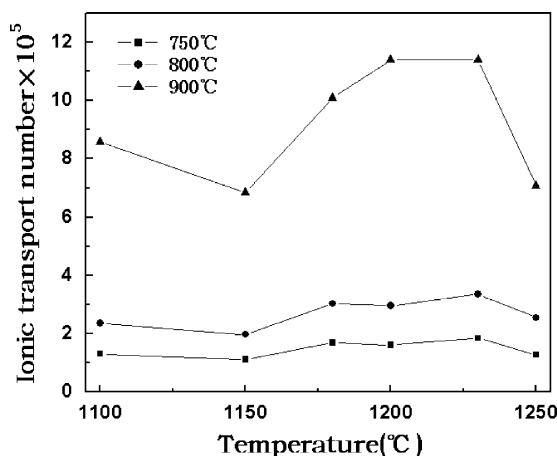


Fig. 6. Oxygen ionic transport numbers of $\text{La}_{0.6}\text{Sr}_{0.4}\text{Co}_{0.8}\text{Fe}_{0.2}\text{O}_3$ ceramics sintered at different temperatures.

numbers at 900 °C, the oxygen ionic conductivities were obtained by the extrapolation of the Arrhenius lines in Fig. 5. As the measuring temperature is identical, the ionic transport numbers are very similar in magnitude and the specimens sintered at 1180–1230 °C show relatively large values. The ionic transport numbers at 900 °C are approximately one order of magnitude lower than those of other $\text{La}_{1-x}\text{Sr}_x\text{Co}_{1-y}\text{Fe}_y\text{O}_3$ compositions measured at the same temperature [6].

The activation energy for small polaron hopping (E_a) was derived from the linear fit of the plots in Fig. 4 over the low temperature range, while the activation energy for oxygen ionic conduction (denoted as E_{ion}) was calculated from the slopes of the straight lines in Fig. 5. Fig. 7 shows the E_a and E_{ion} of $\text{La}_{0.6}\text{Sr}_{0.4}\text{Co}_{0.8}\text{Fe}_{0.2}\text{O}_3$ ceramics as a function of sintering temperature. The activation energy for small polaron hopping varied slightly in the range of 5.33–5.76 kJ/mol, whereas there is an evident change of the activation energy for ionic conduction with sintering temperature. The variation of the activation energy for ionic conduction with sintering temperature is consistent with that of the ionic conductivity.

It is notable that the microstructural evolution with sintering temperature corresponds well to the variation of the mixed conduction properties of $\text{La}_{0.6}\text{Sr}_{0.4}\text{Co}_{0.8}\text{Fe}_{0.2}\text{O}_3$ ceramics. The increase of sintering temperature promoted the microstructural densification. It benefits the conduction of electrical carriers and is thus responsible for the improvement of the mixed conduction properties with the increased sintering temperature in the range of 1100–1200 °C. The exaggerated grain growth after 1200 °C confirms a considerable increase in the amount of liquid. The presence of liquid during sintering can enhance the mass transport and microstructural densification. Nevertheless, the amorphous phase formed by the liquid is a kind of heterogeneous component in ceramic bulk, blocking the transport of

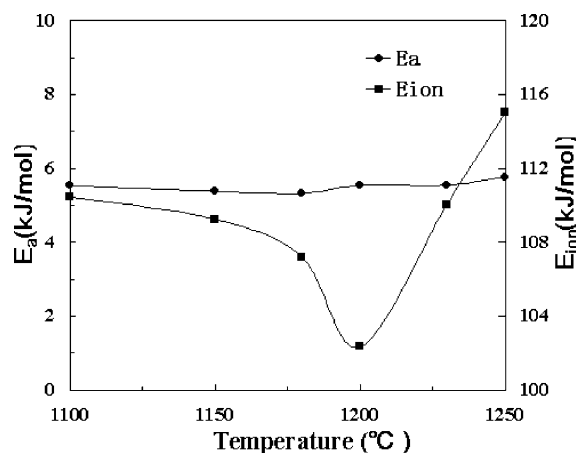


Fig. 7. Activation energy for small polaron hopping (E_a) and activation energy for oxygen ionic conduction (E_{ion}) of $\text{La}_{0.6}\text{Sr}_{0.4}\text{Co}_{0.8}\text{Fe}_{0.2}\text{O}_3$ ceramics as a function of sintering temperature.

electrical carriers. As a result, the degradation of the mixed conduction properties for the specimens sintered at higher temperatures is attributed to the generation of excessive liquid. Therefore, it is crucial to adequately control sintering temperature to achieve desired microstructure and optimum mixed conduction properties. In terms of the mixed conduction properties, it was ascertained that the preferred sintering temperature for $\text{La}_{0.6}\text{Sr}_{0.4}\text{Co}_{0.8}\text{Fe}_{0.2}\text{O}_3$ ceramics is 1200 °C. The specimen sintered at this temperature exhibited an electrical conductivity of $1.26 \times 10^3 \Omega^{-1} \text{cm}^{-1}$ and an oxygen ionic conductivity of $3.73 \times 10^{-2} \Omega^{-1} \text{cm}^{-1}$ at 800 °C.

4. Summary

The influence of sintering temperature on the microstructure and mixed electronic–ionic conduction properties of $\text{La}_{0.6}\text{Sr}_{0.4}\text{Co}_{0.8}\text{Fe}_{0.2}\text{O}_3$ ceramics was investigated in the range 1100–1250 °C. The development of densification at 1100–1200 °C is responsible for the improvement of the mixed conduction properties. Raising the sintering temperature further above 1200 °C resulted in a degradation of the mixed conduction properties due to the generation of excessive liquid. The results demonstrate that it is crucial to adequately control sintering temperature to yield desired microstructure and mixed conduction properties. The preferred sintering temperature was ascertained to be 1200 °C for $\text{La}_{0.6}\text{Sr}_{0.4}\text{Co}_{0.8}\text{Fe}_{0.2}\text{O}_3$ ceramics in terms of mixed conduction properties. The specimen sintered at 1200 °C exhibited an electrical conductivity of $1.26 \times 10^3 \Omega^{-1} \text{cm}^{-1}$ and an oxygen ionic conductivity of $3.73 \times 10^{-2} \Omega^{-1} \text{cm}^{-1}$ at 800 °C.

Acknowledgements

One of the authors (Qing Xu) is grateful to Chonbuk National University for providing a post-doctoral researcher fellowship. This work was financially

supported by the Natural Science Foundation of Hubei Province of China (Grant No. 2001ABB075) and the Foundation for Excellent Youths of Wuhan City of China (Grant No. 20015005031). The State Key Laboratory of Advanced Technology for Materials Synthesis and Processing also provided partial financial support for this work.

References

- [1] Y. Teraoka, T. Nobunage, K. Okamoto, N. Miura, N. Yamazoe, Influence of constituent metal cations in substituted LaCoO_3 on mixed conductivity and oxygen permeability, *Solid State Ionics* 48 (3–4) (1991) 212–270.
- [2] S.J. Beson, D. Waller, J.A. Kilner, Degradation of $\text{La}_{0.6}\text{Sr}_{0.4}\text{Fe}_{0.8}\text{Co}_{0.2}\text{O}_{3-\delta}$ in carbon dioxide and water atmospheres, *J. Electrochem. Soc.* 146 (4) (1999) 1305–1309.
- [3] C.Y. Tsai, A.G. Dixon, Y.H. Ma, W.R. Moser, M.R. Pascucci, Dense perovskite, $\text{La}_{1-x}\text{A}'_x\text{Fe}_{1-y}\text{Co}_y\text{O}_{3-\text{Delta}}$ ($\text{A}' = \text{Ba}, \text{Sr}, \text{Ca}$), membrane synthesis, applications, and characterization, *J. Am. Ceram. Soc.* 81 (6) (1998) 1437–1444.
- [4] L.W. Tai, M.M. Nasrallah, H.U. Anderson, D.M. Sparlin, S.R. Sehlin, Structure and electrical properties of $\text{La}_{1-x}\text{Sr}_x\text{Co}_{1-y}\text{Fe}_y\text{O}_3$. Part 1. The system $\text{La}_{0.8}\text{Sr}_{0.2}\text{Co}_{1-y}\text{Fe}_y\text{O}_3$, *Solid State Ionics* 76 (3–4) (1995) 259–271.
- [5] L.W. Tai, M.M. Nasrallah, H.U. Anderson, D.M. Sparlin, S.R. Sehlin, Structure and electrical properties of $\text{La}_{1-x}\text{Sr}_x\text{Co}_{1-y}\text{Fe}_y\text{O}_3$. Part 2. The system $\text{La}_{1-x}\text{Sr}_x\text{Co}_{0.8}\text{Fe}_{0.2}\text{O}_3$, *Solid State Ionics* 76 (3–4) (1995) 273–283.
- [6] J.W. Stevenson, T.R. Armstrong, R.D. Carneim, L.P. Pederson, W.J. Weber, Electrochemical properties of mixed conducting perovskites $\text{La}_{1-x}\text{M}_x\text{Co}_{1-y}\text{Fe}_y\text{O}_{3-\delta}$ ($\text{M} = \text{Sr}, \text{Ba}, \text{Ca}$), *J. Electrochem. Soc.* 143 (9) (1996) 2722–2729.
- [7] C.C. Chen, M.M. Nasrallah, H.U. Anderson, Impedance response of $\text{La}_{0.6}\text{Sr}_{0.4}\text{Co}_{0.2}\text{Fe}_{0.8}\text{O}_3$ based electrochemical cells, *J. Electrochem. Soc.* 142 (2) (1995) 491–496.
- [8] B.C.H. Steele, J.M. Bae, Properties of $\text{La}_{0.6}\text{Sr}_{0.4}\text{Co}_{0.2}\text{Fe}_{0.8}\text{O}_{3-x}$ (LSCF) double layer cathodes on gadolinium-doped cerium oxides (CGO) electrolytes. II. Role of oxygen exchange and diffusion, *Solid State Ionics* 106 (3–4) (1998) 255–261.
- [9] W. Weston, I.S. Metcalf, $\text{La}_{0.6}\text{Sr}_{0.4}\text{Co}_{0.2}\text{Fe}_{0.8}\text{O}_3$ as an anode for direct methane activation in SOFCs, *Solid State Ionics* 113–115 (1998) 247–251.
- [10] S.R. Wang, T. Kato, S. Nagata, T. Honda, T. Kaneko, N. Iwashita, M. Dokiya, Performance of a $\text{La}_{0.6}\text{Sr}_{0.4}\text{Co}_{0.8}\text{Fe}_{0.2}\text{O}_3\text{-Ce}_{0.8}\text{Gd}_{0.2}\text{O}_{1.9}\text{-Ag}$ cathode for ceria electrolyte SOFCs, *Solid State Ionics* 146 (3–4) (2002) 203–210.